Electronic Supplementary Material (ESI) for Chemical Communications.

Supporting Information

MnFe Phosphides doped in Hollow Prussian Blue Analogues with Ru Modification as Efficient Cathode for Li–O_2 Batteries

Yiru Ma,[‡a] Huiqi Qu,[‡d] Huimin Zhao,[a] Wenna Wang,[a] Xiaolong Li,[b] Yuan Li,[b] Minge Tian,[e] Zhiguo Lv,[d] Yueqin Yu,[a] Bin Li,[*b] Ziyang Guo,[*a] and Lei Wang[*a, c]

a College of Chemistry and Molecular Engineering, State Key Laboratory Base of Eco-Chemical Engineering, International Science and Technology Cooperation Base of Eco-Chemical Engineering and Green Manufacturing, Qingdao University of Science and Technology, Qingdao 266042, PR China.

b College of Materials Science and Engineering, Qingdao University of Science and Technology, Qingdao 266042, PR China.

c College of Environment and Safety Engineering, Qingdao University of Science and Technology, Qingdao 266042, PR China.

d College of Chemical Engineering, Qingdao University of Science and Technology, Qingdao 266042, PR China

e Scientific Green (Shandong) Environmental Technology Co. Ltd, Jining Economic Development Zone, Shandong Province, 272499, PR China

** Corresponding author. Tel & Fax: 0086-0532-84023409*

E-mail address: inorchemwl@126.com (Wang L); zyguo@qust.edu.cn (Guo Z) binli@qust.edu.cn (Li B)

‡Yiru Ma and Huiqi Qu contributed equally to this work.

Experimental Section

Materials. Deionized (DI) water from Milli-Q integral water purification system (Millipore, 18.2 MΩ·cm^{-1}), sodium citrate dihydrate ($C_6H_5NaO_7·2H_2O$, 99.00%, Aladdin), ethyl alcohol (C_2H_6O, AR, Sinopharm Chemical Reagent Corp.), Celgard 2400 (Kejing), polyvinylidene fluoride (PVDF, Kejing), N-methyl-2-pyrrolidone (NMP, 99.9%, Aladdin), potassium ferricyanide ($K_3[Fe(CN)_6]$, 99.50%, AR, Aladdin), tetraethylene glycol dimethyl ether (TEGDME, 99.9%, Aladdin), LiTFSI ($CF_3SO_2NLiSO_2CF_3$, 99.95%, Aladdin). Li foils (15.6 Dia×0.65 mm T, 99.9 %, Shanghai anlu material co., LTD), Ketjenblack (EC600JD, Shanghai Tengmin Industry Co., Ltd.), $RuCl_3•xH_2O$ (35-40% Ru basis, Aladdin), manganese (II) nitrate tetrahydrate ($Mn(NO)_3·4H_2O$, 98%, Aladdin), Carbon paper (TGP-H-060), $NaH_2PO_2·H_2O$ (99%, Aladdin), ethylene glycol ($C_2H_6O_2$, AR, Sinopharm Chemical Reagent Corp.). All chemicals were directly used without further purification.

Preparation of MnFe PBA: The first step of the procedure was to dissolve $Mn(NO)_3·4H_2O$ (0.6 mmol) and $C_6H_5NaO_7·2H_2O$ (0.9 mmol) in 30 mL deionized (DI) water (donated as solution A). $K_3[Fe(CN)_6]$ (0.4 mmol) were dispersed in 30 mL DI water to generate solution B. Afterwards, the solution B was added into the solution A with stirring vigorously for 10 min. Subsequently, the obtained mixture aged for 24h at a room temperature. Finally, the sediment was centrifuged and washed by water and ethanol for several times. Dry at 60 °C in vacuum drying oven to get final product MnFe PBA.

Preparation of Ru-MnFe PBA: The prepared MnFe PBAs (100 mg) were dispersed in 30 mL ethanol through ultrasonic treatment to obtain homogeneous solution. Afterwards, 15 mg $RuCl_3·xH_2O$ was added in the above suspension with magnetic stirring at 60 °C for 2 h. The mixed solution was transferred to an autoclave and maintained for 10 h under high temperature (120 °C). Finally, Ru-MnFe PBA was washed by ethanol and further dried.

Preparation of Ru-MnFeP/PBA: Typically, $NaH_2PO_2·H_2O$ and as-prepared Ru-MnFe PBA were placed in the upstream and downstream of the N_2 flow in tube furnace with mass ratio of 1:30, respectively. Subsequently, the furnace was annealed for 2 h at 350 °C with 5°C min^{-1} heating rate. Upon cooling down naturally, Ru-MnFeP/PBA was synthesized.

Assembly of the Li–O_2 batteries and electrochemical measurements. All the batteries were assembled in a glove box with pure argon ($O_2 < 0.01$ ppm and $H_2O < 0.01$ ppm). The detailed operations were as follow. Ru-MnFeP/PBA catalyst was used as O_2 cathode (12 mm) and Li metal (15.6 mm) was used as anode. The Celgard 2400 membrane of 18 mm was used for separate cathode/anode. 1 M tetraethylene glycol dimethyl ether (TEGDME)/bis (trifluoromethane) sulfonamide lithium salt (LiTFSI) is blended electrolyte. The amount of electrolyte used in each cell was ~0.03 mL. There is an opening with ~ 0.8 cm^2 area on the cathodic side of the Swagelok cell, which guarantees O_2 to enter and participates in the reactions of cathode. The cycling tests and rate capability tests were executed by LAND battery system (Wuhan Land Electronic Co. Ltd., China). Cyclic voltammetry (CV) was carried out by an electrochemical workstation (CHI660D) under scanning rates of 0.1 mV s^{-1} between 2.0 and 4.5 V.

Preparation of Ru-MnFeP/PBA and Ru-MnFe PBA cathodes. Usually, 80 wt% Ru-MnFeP/PBA or Ru-MnFe PBA, 10 wt% KB and 10 wt% polyvinylidene fluoride binder (PVDF) are intimately mixed in NMP. Then, the above uniform slurry was coated on carbon paper (12 mm). To remove residual solvent, the coated electrodes were dried under vacuum at 80°C for 10 hours. The current and specific capacity are calculated based on the mass of Ru-MnFeP/PBA of the cathode. The average mass loading of active material in each electrode was controlled to be 0.2~0.3 mg·cm^{-2}.

Preparation of recharged and discharged Ru-MnFeP/PBA cathodes. The $Li-O_2$ batteries with Ru-MnFeP/PBA cathodes were fully discharged and fully charged at specific programs, respectively. After that, the electrodes of the cells were disassembled in a glove box and cleaned 5 times with dimethoxyethane (DME) until no electrolyte remains. Dry under vacuum at room temperature for 10 hours to get the discharged/charged electrodes.

Physical characterization. X-ray diffraction (XRD) measurements were conducted on a Rigaku-D/MAX/2500PC instrument (Japan). Transmission electron microscopy (TEM) and high-resolution electron microscopy (HRTEM) were characterized by a JEM-2100UHR microscope (Japan). Scanning electron microscopy (SEM) investigations were examined by using Hitachi regulus-8100 (Japan). X-ray photoelectron spectroscopy (XPS) was measured via Kratos AXIS SUPRA (UK) using an Al anode as source with C 1s at 284.6 eV as reference standard to revise the binding energy. Nitrogen sorption measurements were measured at 77 K with a MicroActive ASAP 2460 Version 2.01 (USA). *In-situ* DEMS was conducted using a commercial quadrupole mass spectrometer (Pfeiffer Vacuum, ThermoStar). A quadrupole mass spectrometer (NETZSCH QMS 403 C) with leak inlet was connected to a customized Swagelok cell assembly for DEMS investigation

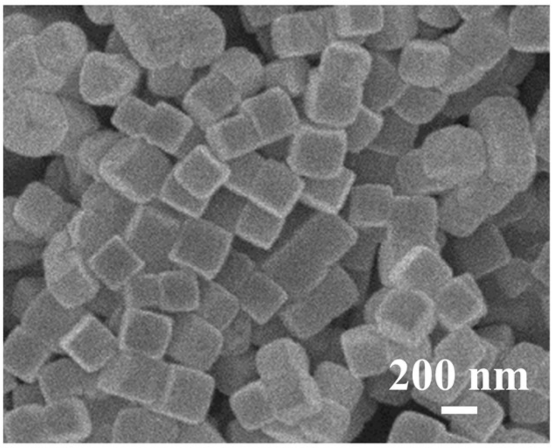

Fig. S1. SEM image of MnFe PBA.

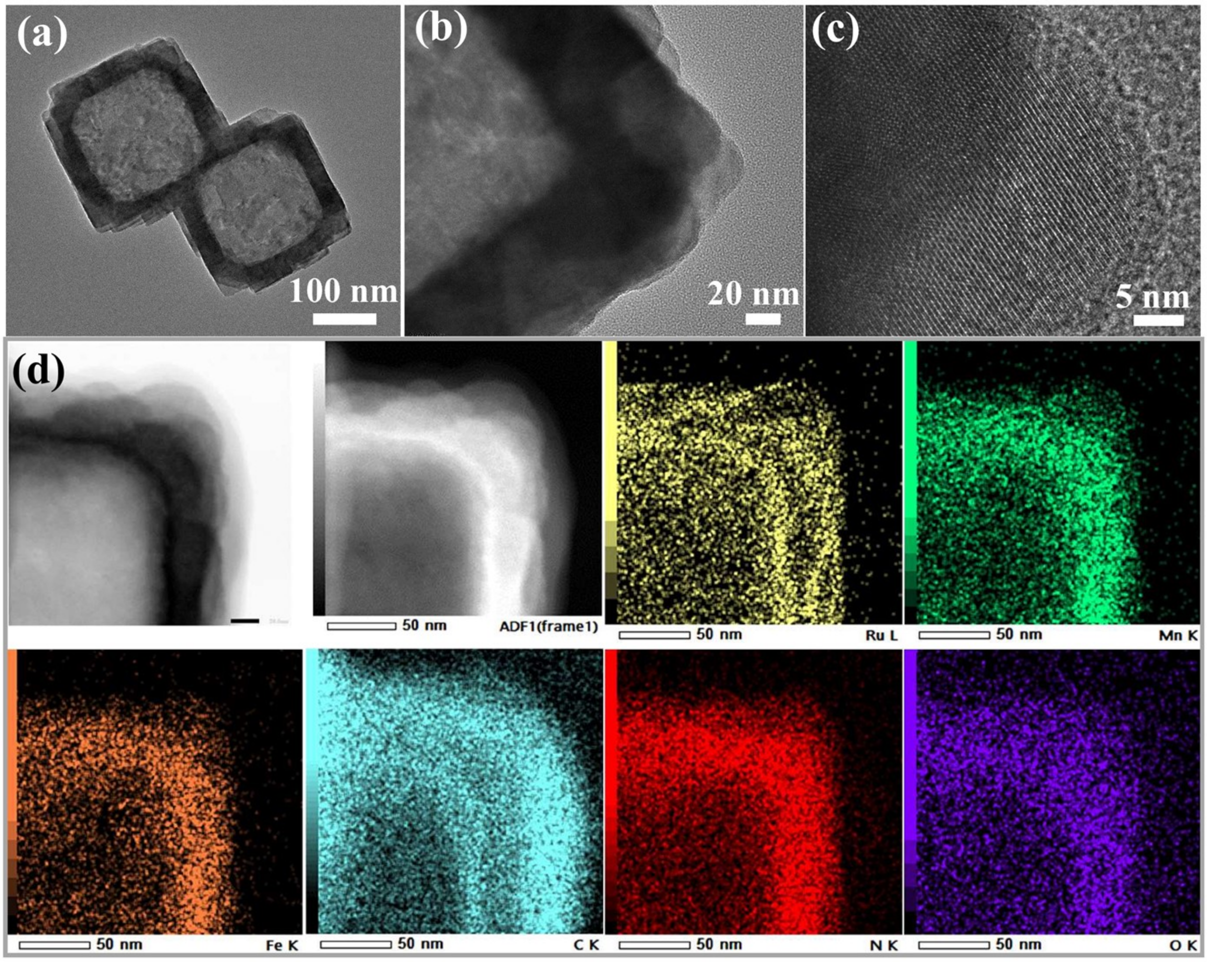

Fig. S2. (a) TEM image and (b-c) HR-TEM images of Ru-MnFe PBA. (d) The relevant EDX mapping images of Ru, Mn, Fe, C, N and O elements, respectively.

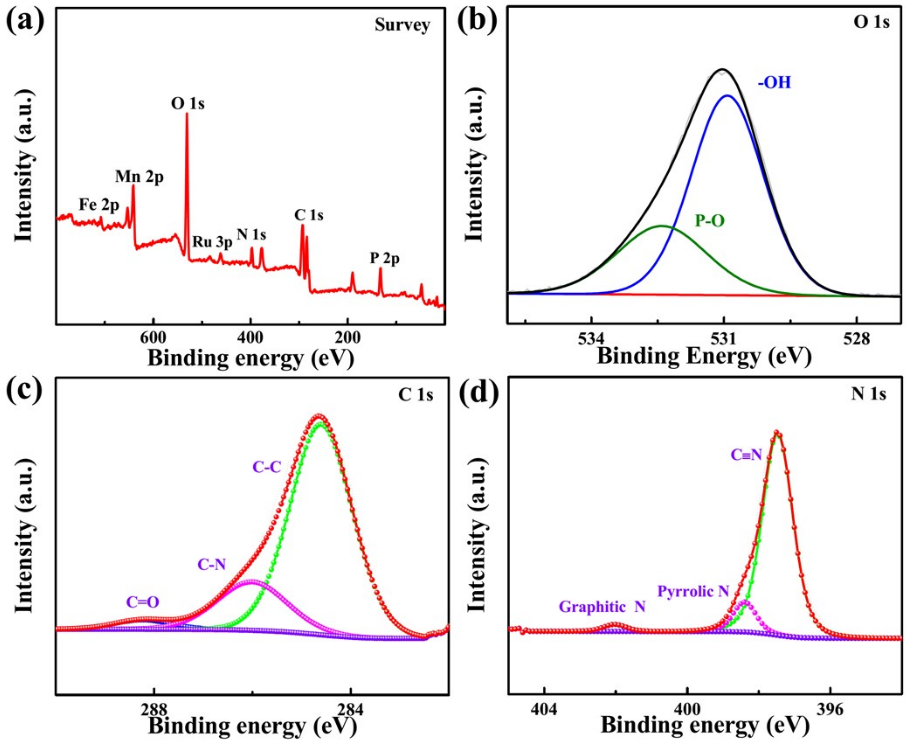

Fig. S3. (a) The full XPS spectrum and the high-resolution XPS spectra of (b) O 1s, (c) C 1s, and (d) N 1s for Ru-MnFeP/PBA.

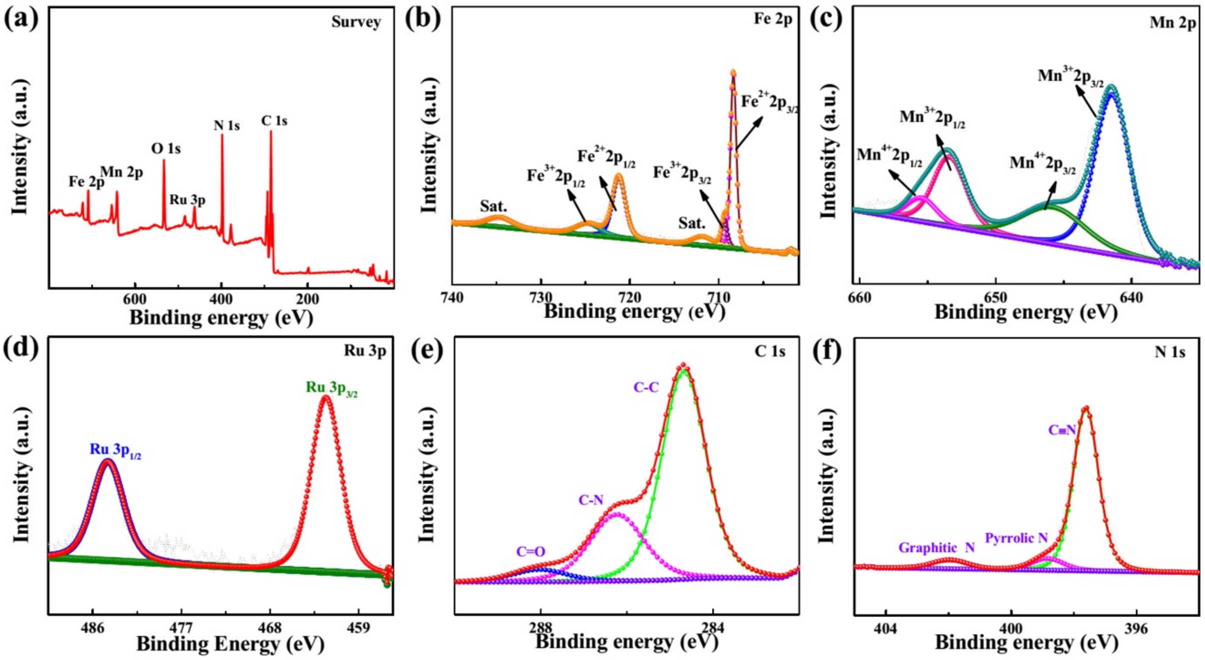

Fig. S4. (a) The full XPS spectrum and the high-resolution XPS spectra of (b) Fe 2p, (c) Mn 2p, (d) Ru 3p, (e) C 1s and (f) N 1s for Ru-MnFe PBA.

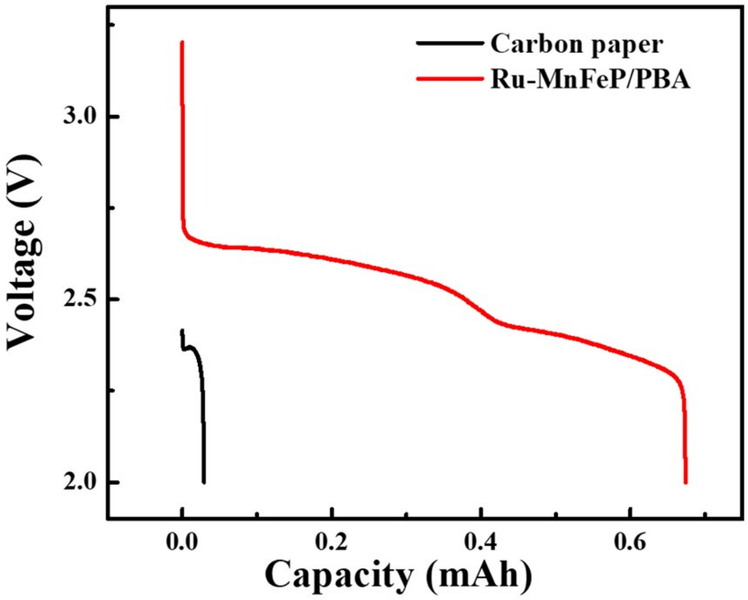

Fig. S5. Discharge curves of the Li−O_2 batteries using the blank carbon paper and the Ru-MnFeP/PBA electrodes at a current density of 0.05 mA cm^{-2}.

The capacity of the carbon paper is quite limited of ~ 0.027 mAh cm^{-2}, which is much lower than that of the Ru-MnFeP/PBA cathode of ~ 0.68 mAh cm^{-2}. The carbon paper as the base of the electrode makes virtually no contribution to the capacity of the electrode.

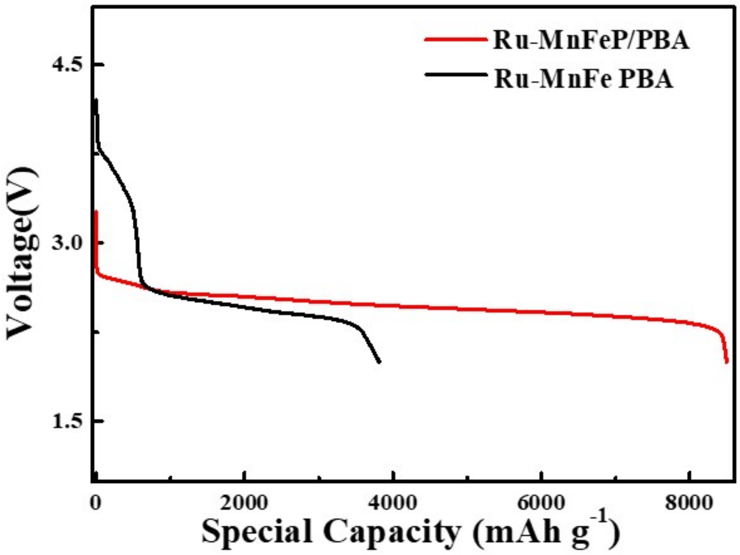

Fig. S6. Full discharge curves of the Ru-MnFe PBA and Ru-MnFeP/PBA electrodes at a current density of 500 mA g^{-1}.

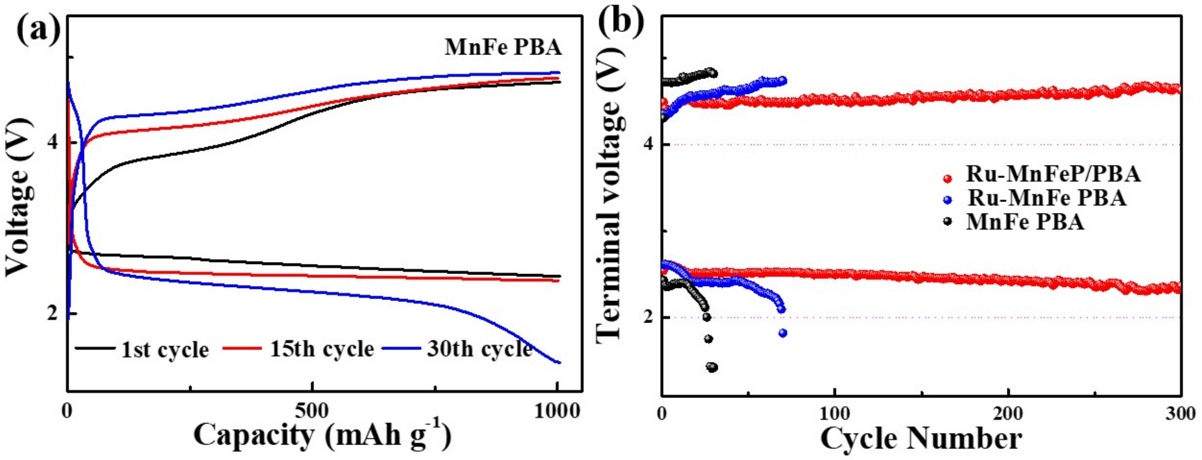

Fig. S7. (a) MnFe PBA cathode at 500 mA g^{-1} with fixed capacity of 1000 mAh g^{-1}. (b) Terminal voltages *versus* the cycle number of three cathodes based batteries.

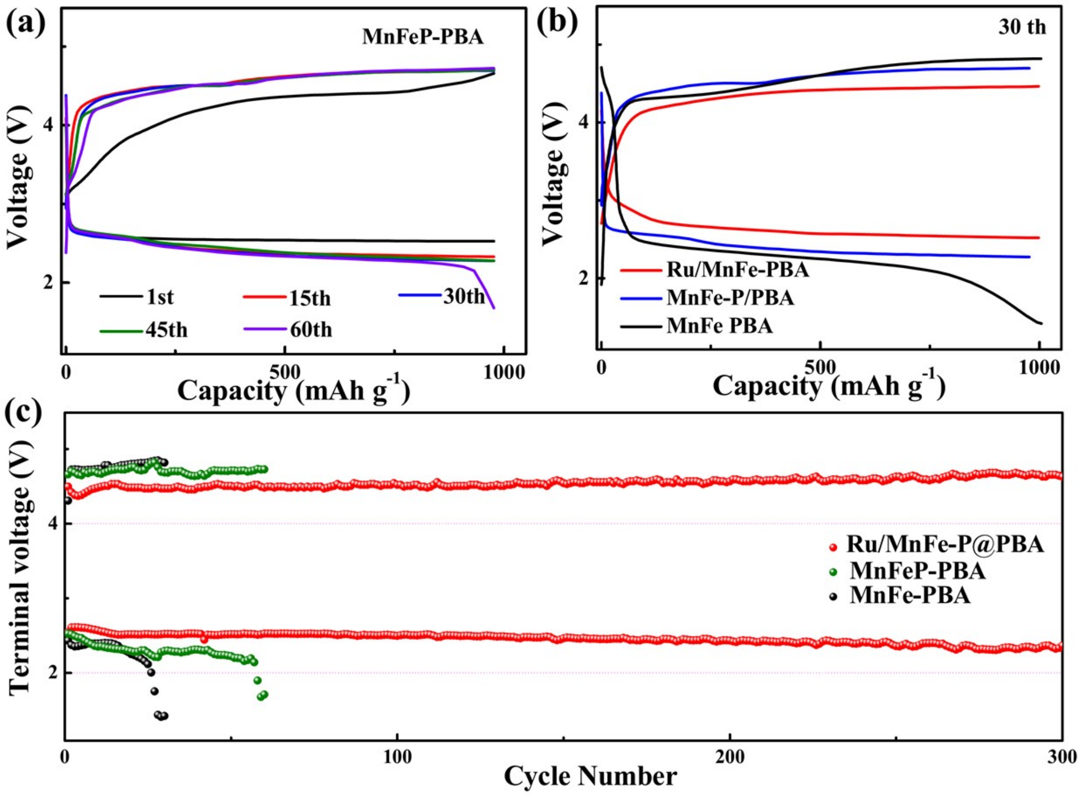

Fig. S8. (a) MnFeP/PBA cathode at 500 mA g^{-1} with fixed capacity of 1000 mAh g^{-1}. (b) The comparison of 30th discharge/charge profiles with Ru-MnFeP/PBA, MnFeP/PBA and MnFe PBA samples. (c) The corresponding terminal voltages *versus* the cycle number of batteries.

MnFeP/PBA was prepared by the similar synthesis process of Ru-MnFeP/PBA (obtained by direct phosphating of MnFe PBA precursor). As shown in Fig. S8a, the Li–O_2 battery using MnFeP/PBA cathode shows the apparent decay after 60 cycles with large voltage gap of 2.99 V. Fig. S7a exhibits that the Li–O_2 battery using the MnFe PBA cathode only be normally operated for 30 cycles, which is much lower than the MnFeP/PBA cathode. The discharge-charge curves of Li–O_2 batteries at 30th cycle is elucidated in Fig. S8b to further reveal the electrochemical performance of different electrodes. The charge platform of Ru-MnFeP/PBA cathode (4.42 V) is lowest among Ru-MnFeP/PBA, MnFeP/PBA and MnFe PBA samples during the 30th cycle. Interestingly, the platform of charging stage with MnFeP/PBA (4.68 V) is smaller than that of MnFe PBA cathode (4.79 V). The results show that Ru-MnFeP/PBA containing ruthenium nanoparticles can promote oxygen reduction more than MnFeP/PBA and pure MnFe PBA catalysts. Moreover, there is no significant degradation of terminal discharge voltage up to 250 cycles for the Ru-MnFeP/PBA electrode and the corresponding cells can perform over 300 cycles. The overpotentials between terminal discharge and charge voltage of the Ru-MnFeP/PBA sample are always the lowest and maintain a steady trend among the three cathodes, demonstrating the superior stability of Ru-MnFeP/PBA cathode in Li–O_2 battery. After 60 cycles, the terminal discharge voltage of MnFeP/PBA electrode decreases to 2 V. In sharp contrast, for the MnFe PBA electrode, the terminal discharge voltage starts to dramatically decrease from the 25th cycle and can only maintain for 30 cycles (Fig. S8c). These above results further prove that the synergy of the highly dispered Ru and metal phosphides nanoparticles in Ru-MnFeP/PBA effectively improves the revesible formation/decomposition of Li_2O_2 in Li–O_2 batteries.

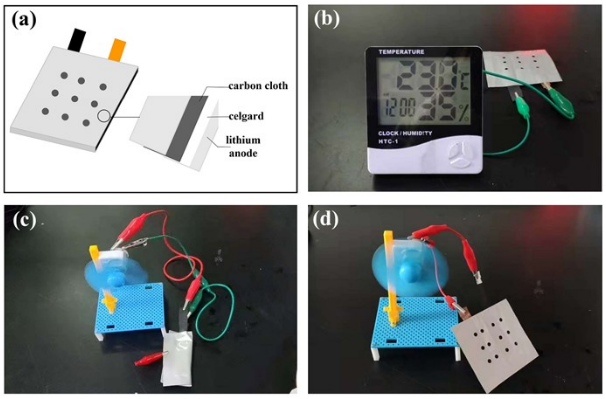

Fig. S9. (a) The diagram of air permeable pouch-type cell. (b) The photograph of the watch powered by the pouch-type cell with Ru-MnFeP/PBA. The photographs of the fan powered by the battery when (c) 180° bending and (d) pristine states.

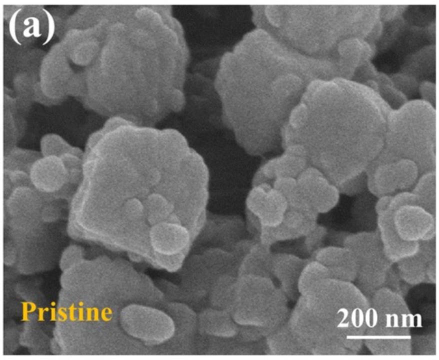

Fig. S10. *Ex-situ* SEM image of the Ru-MnFeP/PBA cathode at pristine stage.

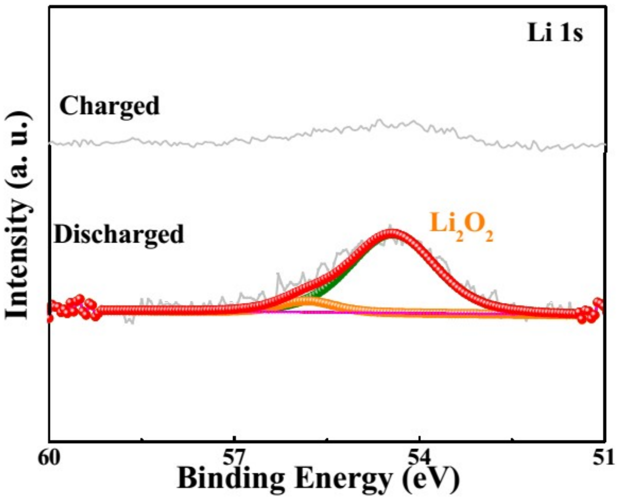

Fig. S11. XPS spectra of Li 1s of the discharged and charged Ru-MnFeP/PBA based electrodes.

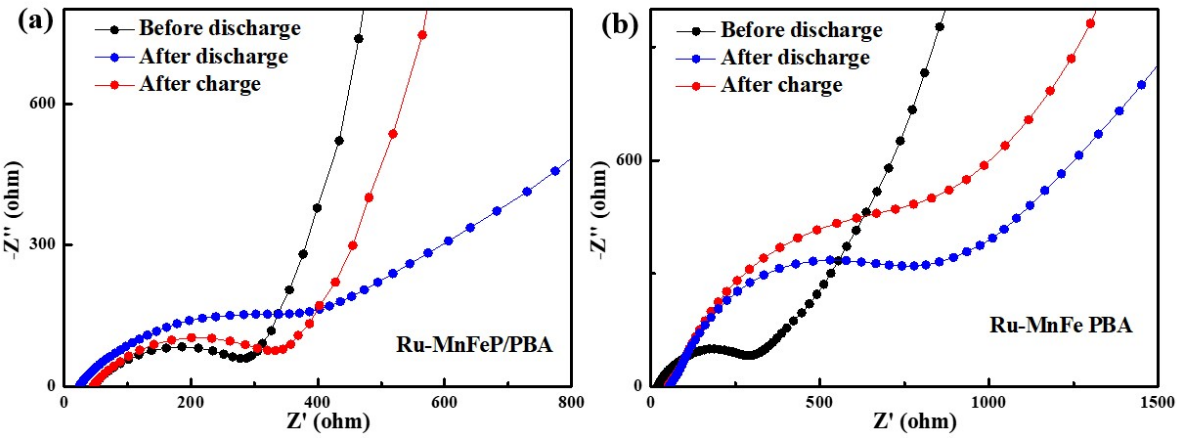

Fig. S12. The comparison of EIS curves with Ru-MnFeP/PBA and Ru-MnFe PBA based Li–O_2 batteries at different stages.

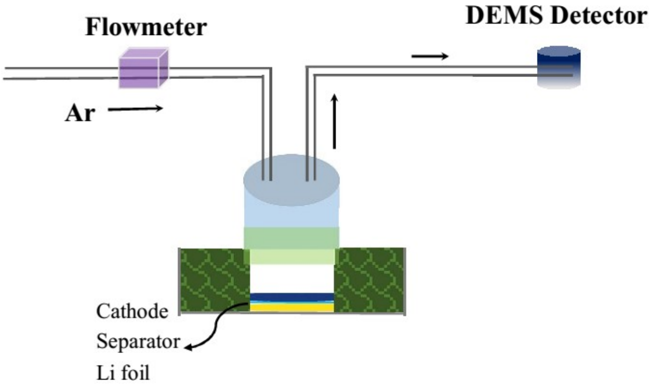

Fig. S13. Schematic illustration of the DEMS analysis system.

The system is guided by the requirement to detect the gases evolved during cycling. A quadrupole mass spectrometer with leakage inlet is connected to a customized Swagelok cell assembly (Fig. S13). The cathode current collector is integrated with two tubes as purge gas inlet and outlet. In the analysis of gas evolution in Li–O_2 battery over charge, pure Ar flow was used for purification. The purification time is 6 hours and the O_2 and O_2 backgrounds are calibrated.

Tab. S1. ICP-OES results of Ru-MnFeP/PBA with different elements.

Elements	contents (wt%)
Ru	4.2
P	7.2